



## Phylogenetic clustering increases with succession for lianas in a Chinese tropical montane rain forest

Mareike Roeder, Michael McLeish, Philip Beckschäfer, Marleen de Blécourt, Ekananda Paudel, Rhett D. Harrison and Ferry Slik

*M. Roeder (mareike@xtbg.org.cn) and M. McLeish, Xishuangbanna Tropical Botanical Garden, Chinese Academy of Sciences, Plant Geography Lab, Menglun, Yunnan 666303, China. – P. Beckschäfer, Chair of Forest Inventory and Remote Sensing, Georg-August-Univ. Göttingen, Büsgenweg 5, DE-37077 Göttingen, Germany. – M. de Blécourt, Soil Science of Tropical and Subtropical Ecosystems, Büsgen Inst., Georg-August-Univ. Göttingen, Büsgenweg 2, DE-37077 Göttingen, Germany, and Inst. of Soil Science, CEN, Univ. Hamburg, Allende-Platz 2, DE-20146 Hamburg, Germany. – E. Paudel and R. D. Harrison, World Agroforestry Centre, East Asia Node, Heilongtan, Kunming 650201, China, and Key Laboratory for Plant Biodiversity and Biogeography of East Asia (KLPB), Inst. of Botany, Kunming 650201, China. – F. Slik, Faculty of Science, Univ. Brunei Darussalam, Jln. Tungku Link, Gadong, BE1410, Brunei Darussalam.*

Previous research found that phylogenetic clustering increased with disturbance for tropical trees, suggesting that community assembly is mainly influenced by abiotic factors during early succession. Lianas are an important additional component of tropical forests, but their phylogenetic community structure has never been investigated. Unlike tropical trees, liana abundance is often high in disturbed forests and diversity can peak in old secondary forest. Therefore, phylogenetic structure along a disturbance gradient might also differ from tropical tree communities. Here we determined phylogenetic community structure of lianas along a disturbance gradient in a tropical montane forest in China, using the net relatedness index (NRI) from 100 equivalent phylogenies with varying branch length that were constructed using DNA-barcode sequences. Three additional phylogenetic indices were also considered for comparison. When NRI was used as index phylogenetic clustering of liana communities decreased with decreasing tree basal area, suggesting that liana competitive interactions dominate during early succession, which is in contrast to the pattern reported for trees. Liana communities in mature forests, on the other hand, were phylogenetic clustered, which could be caused by dispersal limitation and/or environmental filtering. The three additional phylogenetic indices identified different, sometimes contradicting predictors of phylogenetic community structure, indicating that caution is needed when generalizing interpretations of studies based on a single phylogenetic community structure index. Our study provides a more nuanced picture of non-random assembly along disturbance gradients by focusing on a non-tree forest component.

The integration of phylogenetic data in the analysis of communities enables a deeper understanding of what affects community species composition. In these analysis species are not only regarded as an independent unit, but their evolutionary relatedness is also taken into account (Felsenstein 1984, Webb 2000). Species in a community can be phylogenetically more closely (clustered community) or distantly related (overdispersed community) than expected by chance (Webb et al. 2002). Based on the assumption that traits are evolutionary conserved, closely related species should be ecologically and physiologically similar, and therefore share a similar niche. If the environment drives the assembly, more similar species should co-occur (environmental filtering). In contrast, biotic interactions like competition for resources or pathogen pressure should result in dissimilar species co-occurring (biotic filtering) (Webb 2000, Webb et al. 2002). The interpretation of phylogenetic patterns becomes more complicated and ambiguous when additional factors are considered: traits can evolve convergently;

interaction between closely related species can be positive and biotic- and environmental filtering can act simultaneously in a community (Webb et al. 2002, Kembel 2009).

The phylogenetic community structure of climax communities, including forests, has been studied for over a decade (Webb 2000). However disturbed communities have only recently received attention (Verdú and Pausas 2007, Helmus et al. 2010). Disturbance gradients provide opportunities for testing the relative influence of biotic and abiotic factors on assembly processes during succession. Studies of disturbed communities of plankton in lakes (Helmus et al. 2010), old field vegetation (Dinnage 2009) and fire prone shrub lands (Verdú and Pausas 2007) suggests that strong disturbance leads to phylogenetically clustered communities, suggesting that abiotic factors predominantly shape community assembly. Several studies of trees in tropical forests also found clustered communities in strongly or medium disturbed habitats and a decline in relatedness among tree species with ongoing succession (Letcher et al. 2012, Norden et al. 2012, Whitfeld

et al. 2012, Mo et al. 2013). However in other successional forests the opposite trend (Uriarte et al. 2010, Kunstler et al. 2012), constant overdispersion (Letcher 2010), or no phylogenetic pattern (Swenson et al. 2012) was found.

Studies of forest succession and phylogeny have so far focused on trees, whereas we examined liana communities. Lianas form an important component of most tropical forests and influence forest dynamics and productivity by affecting tree growth and regeneration through above and belowground competition (Schnitzer and Bongers 2002). Lianas are often referred to as a disturbance loving growth form. High stem densities from disturbed or high light environments, such as forest edges, tree fall gaps, and secondary forest are frequently reported (Dewalt et al. 2000, Schnitzer et al. 2000, Laurance et al. 2001, Letcher and Chazdon 2009). However, liana diversity and biomass do not necessarily peak in disturbed areas: Liana diversity peaks in older secondary forests, and old growth forests tend to have similar or lower liana diversity than older secondary forests (Dewalt et al. 2000, Letcher and Chazdon 2009). Lianas may gain more importance in the future, since their abundance is likely to increase when primary forests are converted into secondary forest. Moreover, liana abundance also appears to increase in old growth forest, possibly due to climatic changes (Schnitzer and Bongers 2011). As lianas have different life histories compared to trees, the phylogenetic structure of the liana community may reveal different patterns from those of trees, and thus provide a more complete picture of how the community assembly processes vary with succession for different plant groups.

We studied liana communities in a tropical montane forest in southwest China over a wide range of successional phases, from young secondary regrowth to almost pristine forest. Based on the above mentioned phylogenetic studies and liana surveys in successional systems, we predicted a unimodal community phylogenetic pattern (clustered, overdispersed, clustered) along the disturbance gradient. Community phylogenies of lianas should be clustered in young regenerating forest, since strong disturbance can have a detrimental effect also on liana communities, and therefore environmental filtering should influence assembly. In lightly disturbed forests we anticipated phylogenetically overdispersed communities because relatively favorable growing conditions should result in competition for resources. High canopy closure in old growth forests is expected to lead to phylogenetic clustered liana communities, because high canopies and shade could be a strong environmental filter. To test this hypothesis, we used sequence data from DNA barcodes to improve the identification of lianas and to construct a phylogeny that incorporated all species and morphospecies in the community. Since the detection of phylogenetic patterns depends highly on the phylogenies used (Webb et al. 2002), and phylogenetic reconstruction generally produces a set of equally likely solutions, we used 100 equally likely phylogenies to account for these uncertainties in branch lengths. To date, this variation is generally ignored, although it could affect the results of analyses considerably (Webb et al. 2002, Kress et al. 2009).

We address the following questions: does the phylogenetic structure of liana communities vary along a disturbance gradient defined by forest structure? Does the phylogenetic

structure of liana communities correlate with environmental variables such as soil characteristics or topography? How does incorporating all optimal solutions of the phylogeny affect the interpretation of community phylogenetic analyses? Do different phylogenetic community structure measures produce corresponding outcomes? Can DNA-barcodes assist in liana identification for field studies?

## Methods

### Study site

Liana communities were surveyed in a montane forest in permanent plots (Making Mekong Connected project, Xu et al. 2014), Mengsong township, Xishuangbanna, Yunnan, China (21°28–34'N, 100°26–31'E). The plots are distributed over an area of approximately 120 km<sup>2</sup> where elevation ranges from 1160 to 1840 m. Mean annual temperature is 18°C and annual precipitation 1600–1800 mm (at 1600 m). Most precipitation (80%) occurs during the monsoon season from May to October (Xu et al. 2009). Soil types varied between Acrisols and Ferralsols (WRB IUSS Working Group 2006). Secondary forest of the area mainly resulted from the succession of swidden cultivated land (Xu et al. 2009). Around 400 tree species were found in the plots, and most abundant were trees of the Lauraceae and Fagaceae families (Zhu et al. 2005, Paudel et al. unpubl.). The canopy forming trees are 25–35 m tall (Zhu et al. 2006).

### Field survey

Twenty-two plots ranging from young regenerating to old-growth forest were selected according to double stratified sampling (Fleischer 1990). First a point grid of 500 × 500 m was laid over the landscape and each point was assigned to open land, regenerating forest, or old-growth forest based on a RapidEye satellite image. The study site was divided into 16 equal area units. One regenerating forest plot and one old-growth forest plot were randomly selected within 12 of these units (Beckschäfer et al. 2013). However, some of the units did not contain any old-growth forest, resulting in a total of 12 regenerating and ten old-growth forest plots (Fig. 1).

Each plot consisted of nine circular subplots (10 m radius) arrayed in a 3 × 3 grid with 50 m distance between subplots (Fig. 1). Data for canopy closure, soil texture and soil nutrients, tree diameter and tree species for trees ≥ 10 cm (10 m radius circle) and trees ≥ 2 < 10 cm diameter (5 m radius circles) were available from surveys conducted in 2010 and 2011 for all plots (Beckschäfer et al. 2013, de Blécourt unpubl., Paudel et al. unpubl.).

All liana stems (≥ 0.5 cm diameter) in the 5 m radius circles of a subplot (707 m<sup>2</sup> per plot, total area = 1.6 ha) were measured and identified during November 2011 to February 2012. Stems and life forms included in the survey followed the liana census protocol (Gerwing et al. 2006, Schnitzer et al. 2008), like e.g. excluding climbing bamboo. We used measurements from liana individuals (apparent genet), ramets (all rooted stems including clones), and basal area per plot in our analyses. Vouchers and DNA samples for each spe-

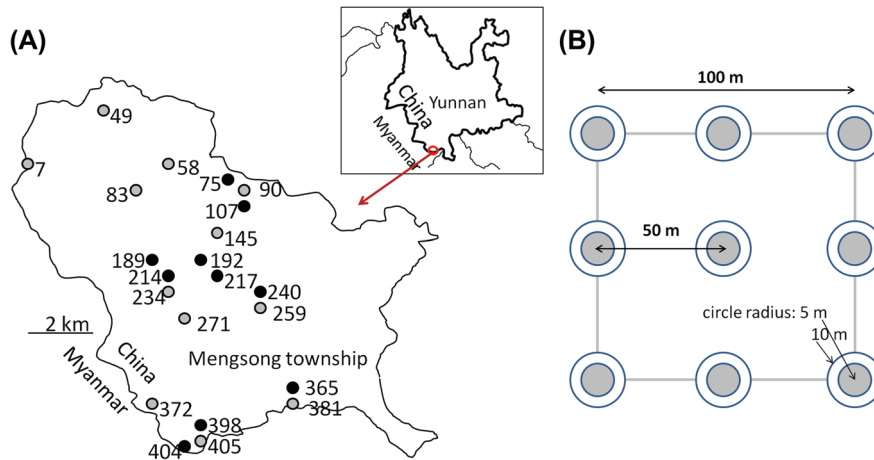


Figure 1. (A) Twenty-two plots were distributed over ~120 km<sup>2</sup> in Mengsong township, Xishuangbanna, Yunnan, close to the border with Myanmar. The distribution was based on stratified sampling in 12 grid cells; dark plots were initially selected as old-growth forest plots, grey as regenerating forest. Plots names are given. (B) Each plot consisted of 9 subplots (B). The liana survey was restricted to the 5 m radius subplots, but soil and forest structural data were sampled from the 10 m radius circles.

cies per plot were collected. When no leaves were available and the liana stem could not be identified in the field, DNA from cambium tissue and a stem photograph were taken. The dried specimens were identified to species or morphospecies level by comparing them with herbarium vouchers from the HITBC herbarium (Xishuangbanna Tropical Botanical Garden). Analysis of basal area, ramet and individual density per plot included all lianas, although for the phylogenetic analysis, *Gnetum monatum* as the only gymnosperm, and all unidentified stems were excluded (total 2% of all ramets).

### DNA extraction, amplification, sequencing

DNA was extracted from 160 dried leaf tissue samples in total, for each of the 127 species 1–4 individuals were used. We sequenced three plastid (*rbcl*, *matK*, *trnH-psbA*) and one nuclear region (*ITS*). For additional 120 liana individuals, where no leaf material was available, DNA was extracted from cambium tissue and the *matK* and *ITS* regions were amplified for sequencing (see below). All extractions were achieved using the DNeasy Plant Mini Kit (Qiagen) following the supplier's protocols. We added polyvinylpyrrolidone (PVP) in the first step (2%) to improve the yield from tissue of several families. The primers (Beijing Dingguo Changsheng Biotechnology) for *rbcl*, *matK*, *trnH-psbA*, *ITS* and PCR protocols used here are described in previous studies (Gonzalez et al. 2009, Kress et al. 2009, Erickson pers. comm.). Primers and protocols including slight modifications are given in the supplementary material (Supplementary material Appendix 1, Table A1, A2). All isolates were sent to BGI (China) for purification and sequencing in both directions (Sanger method).

### Sequence alignment and matrix assembly

Sequences were aligned with Clustal X2.1 (Larkin et al. 2007) and edited by hand in *MEGA5* (Tamura et al. 2011). The reading frames of *rbcl* and *matK* were determined from

amino acid sequences available from Genbank. Each locus (*matK*, *rbcl*) was aligned separately and then concatenated into one matrix with Mesquite ver. 2.7.5 (Maddison and Maddison 2011). Due to the high incidence of insertions and deletions present in the *ITS* and *trnH-psbA* sequence data, we aligned sequences within each family separately and added them to the matrix in a stepwise fashion (Kress et al. 2009). Species that were the only representative of their family were aligned within order. Single representatives of one order could not be aligned, and therefore these *ITS* or *trnH-psbA* sequences were omitted (*Polygonum* sp., *Passiflora wilsonii*, *Rourea minor*). Gaps were coded as missing data. All sequences have been submitted to Genbank (Supplementary material Appendix 1, Table A4).

### Identification of liana stems with *matK/ITS*

Liana stems that could not be reliably identified were barcoded and assigned to species groups using maximum likelihood pairwise distances (K2P) of the *matK* alignment, which included sequences of all cambium and leaf samples (total 280 samples). Sequences were assigned to a species if the K2P pair-wise distance was  $\leq 0.006$ . This threshold was chosen because it was a conservative estimate of intraspecific variation derived from the pair-wise distance curve of *matK*. We estimated pair-wise distances from the *ITS* alignment to clarify ambiguities that arose using the *matK* distance estimates. Queries that did not match any of our database records of *matK* and *ITS* sequences (K2P *matK* > 0.009, K2P *ITS* > 0.03) and had distinctive characters on the stem photographs, were treated as separate 'phylogenetic' species. We sequenced *rbcl* from these species so that three loci were represented for each in the data matrix.

### Phylogenetic tree

We used parsimony and probabilistic approaches to infer phylogenies with RAxML ver. 7.2.8 (Stamatakis 2006), and

MrBayes ver. 3.2.1 (Ronquist et al. 2012). To investigate the contribution of each locus to the trees, the matrix was partitioned per gene. We used the general time reversible (GTR) model in each partition. The backbones of the phylogenies were constrained to order level following the APG III topology (2009). Bayesian inferences were performed over two simultaneous analyses with four Markov chains. Posterior probabilities were sampled every 1000th tree from  $7.5 \times 10^6$  post-burn-in generations. The first 25% of trees were omitted from analysis to assure the chains had reached apparent stationarity. The analysis was applied three times to the dataset to verify convergence of the phylogenetic inferences. Thus in total over 44 000 trees were obtained. We constructed a filter tree based on a majority rule (50%) consensus tree and constrained the topology according to APG III and other published phylogenies on family level (Backlund et al. 2000, Kajita et al. 2001, Livshultz et al. 2007, Zhang et al. 2011). We then filtered the 44 000 post-burn-in posterior trees with our constraint tree for phylogenies with the same topology, but varying branch lengths (136 trees). We randomly picked 100 of these filtered trees, and used them in subsequent analyses. Likelihood analysis was conducted with RAxML using the rapid bootstrap analysis and search for the best-scoring tree using 1000 runs. Three species belonging to the family Schisandraceae were used as outgroup. Schisandraceae was the most basal clade present in our analysis according to APG III. Only one individual with the most complete sequence per species was used in the phylogeny. The single gymnosperm species, *Gnetum montanum* was excluded from the phylogeny. The long branch length connecting Angiosperms and Gymnosperm would have overemphasized the importance of *Gnetum* in communities, resulting in biased relatedness indices based on its presence in a community.

### Phylogenetic community analysis

To assess the phylogenetic structure within communities we calculated the net relatedness index (NRI) with R 2.14.2 (R Development Core Team, Kembel et al. 2010) for each plot. The NRI is based on the mean pair-wise phylogenetic distance of all species pairs in a community (MPD), which is standardized by a MPD calculated from randomized matrices:  $NRI = -1 \times (MPD_{obs} - MPD_{rand}) / SD MPD_{rand}$  (Webb et al. 2002). We used 999 randomizations and a null model that maintained the species and individuals per plot, but randomized species location in the phylogeny. We weighted our NRI using liana ramet abundance ( $NRI_{ramet}$ ) and basal area ( $NRI_{ba}$ ). We included NRI weighted by liana basal area, since positive NRI values are interpreted as biotic interaction, and stem size may be more important than stem number. We calculated the NRI from our Bayesian consensus and the maximum likelihood tree. To account for branch length variation, NRIs of all 100 filtered phylogenies with varying branch lengths were calculated, using the mean of 100 NRI and standard deviation per plot for further analysis. If the species of a community are more closely related than expected by chance, the community is clustered and the NRI positive; a negative NRI indicates phylogenetic overdispersion (Webb et al. 2002). The interpretation of NRI in this study is based on the assumption, that traits are generally

evolutionary conserved (Prinzing et al. 2001). NRI is a widely used, easy to interpret index and therefore comparable with most other studies. Additionally, we calculated NTI (nearest taxon index), PSV (phylogenetic species variability) and PSE (phylogenetic species evenness). NTI is calculated and interpreted similar to NRI, but is based on the mean nearest taxon phylogenetic distance (MNTD) (Webb et al. 2002). PSV is an index similar to NRI (Helmus et al. 2007). It is based on the decrease of variance of a common hypothetical trait that evolves along the phylogeny compared to a star shaped phylogeny. PSE is an abundance weighted PSV and similar to abundance weighted NRI, it decreases with differences in species abundance. PSV and PSE range between 0 and 1, strongly phylogenetic clustered communities have a value close to 0 (Helmus et al. 2007). PSV and PSE therefore have the opposite direction as NRI. PSV and PSE are standardized against a star phylogeny, NRI and NTI against the mean of random communities of the species pool.

### Environmental data and forest structure

The available soil data included concentration of macronutrients (N, P, K), concentration of secondary or micronutrients (Fe, Mn, Ca), soil texture (percentage of sand, clay, silt), pH in H<sub>2</sub>O, and total carbon concentration per subplot (de Blécourt et al. unpubl.). We used means of variables (median for pH) per plot. All soil data were collected at a depth of 0–30 cm. In order to reduce environmental variables for subsequent analyses, a principle component analysis (PCOrd 5.0, MJM software, Glenden Beach, OR, USA) was conducted with 10 soil variables: N, P, K, Ca, Mn, Fe, clay, silt, pH, C/N ratio. Carbon was highly correlated to nitrogen ( $\rho = 0.93$ ,  $p < 0.0001$ ) and sand was correlated to clay ( $\rho = -0.8$ ,  $p < 0.0001$ ) and to iron (Fe) ( $\rho = -0.8$ ,  $p < 0.0001$ ). Carbon and sand were therefore excluded from the PCA. The three first PCA axes, which explained 42, 24 and 11% of variation, were used in further analyses. Axis 1 was associated with micronutrients and clay, axis 2 with nitrogen and potassium, axis 3 with silt, pH and phosphorus.

Four variables were used to describe the forest structure: 1) stem density of trees  $\geq 10$  cm diameter at breast height (DBH); 2) stem density of trees  $\geq 2$  cm  $< 10$  cm DBH; 3) basal area of tree stems  $\geq 10$  cm; and 4) mean canopy closure (percentage) per plot derived from hemispherical photographs (Beckschäfer et al. 2013). Stem density of bamboo (non-climbing and climbing, *Pseudostachyum polymorphum*, *Dendrocalamus spec.*, cf. *Dinochloa sp.*) can be an indicator of disturbance and was therefore also included. Density and basal area was summed per plot. Topographic variables included average slope and elevation per plot.

### Statistical analysis

Ordinary least square (OLS) regression was used to determine the main biotic and abiotic factors (independent variables) that influence liana community structure (response variable). The relationship between response and independent variables was investigated using STATGRAPHICs (Statpoint Technologies, Warrenton, VA, USA). The relationship for

OLS should be either linear or not significant, but not another type. Variables were transformed, if necessary (log transformation – bamboo density, canopy closure; quadratic transformation – tree stem < 10 cm). For the model selection, soil data (soil PCA axis 1–3), forest structure data, and topography were independent variables that could be selected. Model selection was based on calculating OLS models for all possible combinations of the independent variables, after which the models were ranked according to the Akaike information criterion (AIC). Independent variables were included in the linear regression when they occurred in best models with  $\Delta\text{AIC} < 2$ . For the phylogenetic index NRI, one OLS regression was run for the mean value (e.g. mean of 100  $\text{NRI}_{\text{ramet}}$ ) and an additional 100 OLS models were run with phylogenetic indices that were based on the 100 randomly selected filtered phylogenies with identical topologies to account for uncertainties in branch lengths. Response variables and residuals from the OLS were tested for spatial autocorrelation by calculating Moran's I coefficient. Liana structural variables,  $\text{PSE}_{\text{ba}}$ ,  $\text{PSE}_{\text{ramet}}$ ,  $\text{NTI}_{\text{ramet}}$ ,  $\text{NTI}_{\text{ba}}$ ,  $\text{NRI}_{\text{ramet}}$  were not spatially autocorrelated, and less than a quarter of all  $\text{NRI}_{\text{ba}}$  were spatially correlated. Therefore, autocorrelation had a minor influence on the interpretation of the regression coefficients and was ignored. We used a likelihood ratio test to examine if the relation between NRI and correlated forest structural variables were linear or unimodal. Regressions, tests for spatial autocorrelation, and model selection were done with Spatial Analysis for Macroecology ver. 4.0 (Rangel et al. 2010).

To test how phylogenetic patterns depend on the structure of each liana community, we also correlated NRI with liana ramet density, liana basal area, and rarefied liana species richness per plot (Gotelli and Colwell 2001). We used nonmetric multidimensional scaling (NMDS, R package *vegan*, (Oksanen et al. 2013)) to investigate the liana floristic similarity of the plots. The analyses included standardization and square root transformation of the data to avoid problems with zero-inflated matrices (Wisconsin double standardization), Bray–Curtis distance, and an automatic stop of random starting points for the ordination once convergent solutions are found (function *metaMDS*). We used the function *Envfit* to relate the ordination scores to the environmental variables (forest structure, topography, scores of three soil PCA axis, altitude) and plot coordinates. *Envfit* uses regression and assesses the significance by permutation of the response variable (1000 times). Liana vegetation matrix, plot data for forest structure, soil, topography and the 100 used phylogenies are available in Supplementary material Appendix).

## Results

### DNA-barcoding and liana identification

Sequencing success was high across all markers for the tried PCR samples: 93% (*ITS*), 99% (*rbcL*), 98% (*matK*), and 91% (*trnH-psbA*). In total 1126 single sequences were obtained. Ninety-two of 116 (79%) successfully sequenced stem samples could be directly assigned to a species with leaves, having a pairwise distance of zero for the *matK* region.

Eight stem samples had pair-wise distances of 0.003 and 0.006 when compared with identified species and were also assigned to a species. Seven stem samples had zero distance with several species, therefore, the *ITS* region was sequenced in addition to *matK* and enabled species assignment of a further five stems. Nine stem samples had no close fit to any species (distance *matK*  $\geq 0.009$ ,  $\geq 0.03$  *ITS*). These were grouped into five new species and included in the phylogeny. Some stems had very distinct bark features, and so even when genetic distance was low (0.009), morphology justified treating them as separate species.

### Liana density, diversity, and composition patterns

Over 3000 individuals (apparent genets) and over 3800 ramets (individuals and their clones) were measured and identified. Differences in liana density between plots ranged from 38 to 343 individuals, with a mean of 144 individuals per plot (144 in  $0.1 \text{ ha}^{-1}$ ). The mean ramet density per plot was 175 (248 ramets  $0.1 \text{ ha}^{-1}$ ) and highly correlated with liana individual density ( $r = 0.97$ ,  $p < 0.0001$ ). We therefore excluded individual density and used the more reliable ramet data (no subjective distinction of apparent individuals) in subsequent analyses. Mean liana basal area per plot was  $0.9 \text{ m}^2 \text{ ha}^{-1}$  (range  $0.05$ – $1.7 \text{ m}^2 \text{ ha}^{-1}$ ) and was not correlated with individual or ramet density. Fourteen to 39 species were found per plot. A total of 132 species and morphospecies from 39 families were identified. Five of these species had no vouchers, and were only identified from barcodes (Supplementary material Appendix 1, Table A4).

According to the best OLS model, liana ramet density was mainly influenced by soil properties (soil PCA axis 1, micronutrients and clay) and increased with elevation (Table 1). Liana basal area increased with steeper slopes and higher canopy closure, but decreased with increasing basal area of trees (Table 1). However, the negative relationship between tree and liana basal area was mainly driven by one plot of old-growth forest with few lianas. Liana basal area also correlated with soil PCA axis 3 (pH, silt, P). Rarefied liana species richness increased with tree basal area and slope and was correlated with soil PCA axis 2 (N, K) and axis 3 (pH, silt, P) (Table 1).

Liana composition changed along a north-south gradient, with latitude having the strongest correlation with NMDS ordination ( $r^2 = 0.55$ ,  $p = 0.001$ , Fig. 2). Soil PCA axis 3 also correlated with the NMDS ordination ( $r^2 = 0.4$ ,  $p = 0.01$ ) as well as forest structure such as canopy closure, tree stem density ( $> 10 \text{ cm DBH}$ ) and tree basal area (all  $r^2 < 0.36$ ,  $p < 0.05$ ). The NMDS ordination converged on a solution after an average of 14 starting points. Two dimensions were used, the stress was 18.7%.

### Phylogenetic community structure

The NRI values per plot calculated with different phylogenies (maximum likelihood, consensus from Bayesian approach, average NRI from 100 Bayesian phylogenies) were all highly correlated (all comparisons  $r > 0.99$ ,  $p < 0.001$ ). Therefore in the subsequent analysis, only the averaged NRI per plot derived from the 100 NRIs of equally likely alternative

Table 1. Results of ordinary least square model (OLS) selection (based on Akaike information criterion) for liana community structural (density, basal area, and rarified species richness) and phylogenetic data (net relatedness index, NRI). The overall model results (adjusted  $r^2$ , F-ratio, and p-value) and the standardized coefficient and associated p-value for each selected independent variable are given. Transformations of independent variables are indicated in brackets.  $NRI_{ramet}$  and  $NRI_{ba}$  are the weighted NRI value for ramet density and basal area, respectively. OLS models were run for the averaged net relatedness index (NRI) obtained from 100 different, but equally likely phylogenies. In addition, OLS models were run for each of the 100 individual NRI values obtained from each phylogeny and the frequency with which the independent variables were selected is given, as well as the direction of the coefficient.

Independent variable	Response variable											
	liana ramet density		liana basal area		rarified liana species richness		$NRI_{ramet}$		$NRI_{ba}$			
	adj. $r^2$	F	adj. $r^2$	F	adj. $r^2$	F	adj. $r^2$	F	Included in n out of 100 OLS models (direction of coefficient)	adj. $r^2$	F	Included in n out of 100 OLS models (direction of coefficient)
	std coef	p	std coef	p	std coef	p	std coef	p		std coef	p	
tree basal area			-0.464	0.016	0.477	0.018	0.565	0.007	95 (+)	0.423	0.051	64 (+)
tree stem $\geq 10$ cm									2 (+)			
tree stem $\geq 2 < 10$ cm (quadratic)												
canopy closure (log)			0.528	0.006					2 (+)			36 (+)
slope			0.419	0.015	0.368	0.042	0.373	0.046	84 (+)			
elevation	0.534	0.008							5 (+)			32 (-)
soil PCA axis 1	-0.812	<0.001					-0.444	0.02	91 (-)			4 (-)
soil PCA axis 2					-0.41	0.003	-0.489	0.014	95 (-)			39 (-)
soil PCA axis 3			-0.514	0.004	-0.328	0.063			27 (-)			7 (+)
bamboo stems (log + 1)												

phylogenies was used. We also checked if NRI changed when it was weighted by liana ramet or individual abundance: both NRIs were highly correlated ( $r < 0.98$ ,  $p < 0.001$ ), justifying our choice of just using ramet density.

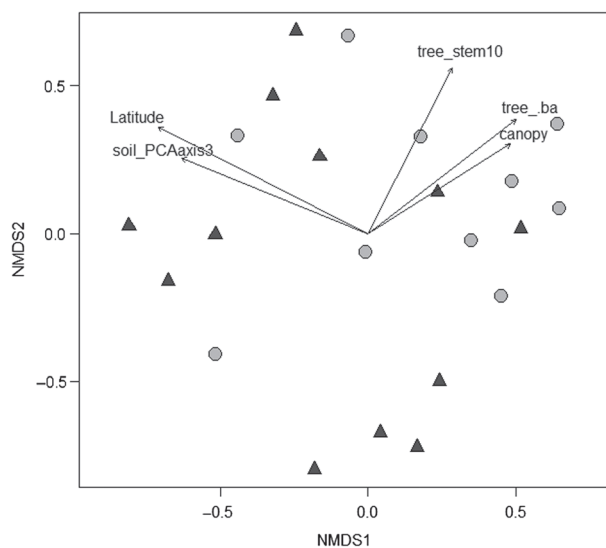


Figure 2. NMDS of liana species composition (ramet abundance) in 22 plots in montane rain forest, SW China. A post hoc correlation with forest structural data, coordinates and topography was done and significant variables ( $p \leq 0.05$ ) are shown. Convergent solution was reached on average after 14 runs, stress was 18.7%. Triangles symbolize regenerating forest plots, circles old growth plots.

NRI was not correlated with liana ramet density. Rarified liana species richness was higher in plots with phylogenetically clustered communities ( $NRI_{ramet}$ :  $r = 0.72$ ,  $p < 0.001$ ,  $NRI_{ba}$   $r = 0.58$ ,  $p = 0.005$ , Fig. 3). Liana basal area also increased with  $NRI_{ramet}$  ( $r = 0.54$ ,  $p = 0.01$ ).

Overall, tree basal area was the most important predictor for NRI: liana communities were phylogenetically more clustered when tree basal area was higher (Table 1; Fig. 4). Slope was positively correlated with  $NRI_{ramet}$ . The negative coefficient for soil PCA axis1 and PCA axis2 means, that  $NRI_{ramet}$  increased with increasing clay and micronutrient content and with decreasing nitrogen content. The OLS model explained 48% of the variation in  $NRI_{ramet}$  between the plots (Table 1). The selection of different predictors based on different  $NRI_{ramet}$  values calculated from the 100 filtered trees was negligible: over 90% of the models included tree basal area and the two PCA soil axes. However, 86% also included slope as a significant predictor.

For  $NRI_{ba}$ , tree basal area was the only predictor in the best model, but explanatory power of the model was low (adjusted  $r^2 = 0.18$ ) (Table 1). The 100 different  $NRI_{ba}$  values from the filtered trees produced different best models: tree basal area and soil PCA axis 2 were selected 68 and 39% respectively, or, canopy closure together with elevation in 36 and 32% of models, respectively. For both,  $NRI_{ba}$  and  $NRI_{ramet}$  a unimodal function did not fit better than a linear one to describe the relation to tree basal area (maximum likelihood ratio test,  $F < 0.41$ ,  $p > 0.5$ ).

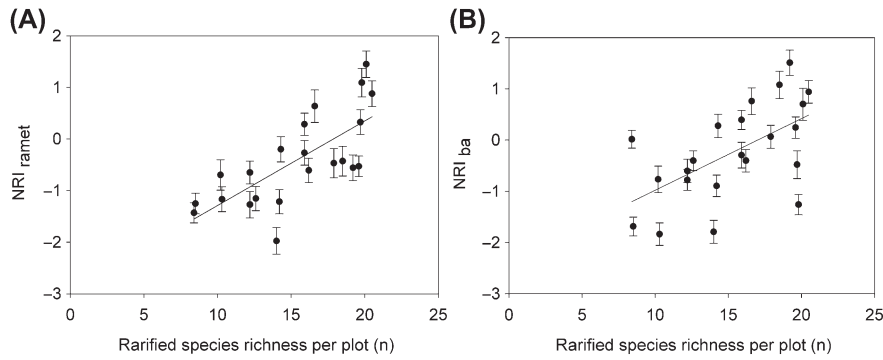


Figure 3. Correlation (Pearson) between rarified liana species richness and net relatedness index (NRI) weighted by ramet density ((A),  $r = 0.72$ ,  $p < 0.001$ ) and basal area ((B),  $r = 0.58$ ,  $p = 0.005$ ). For each plot, 100 NRIs based on 100 phylogenies with different branch length were calculated. Shown are mean and standard deviations. Note: calculation of NRI is independent of species richness.

The additional phylogenetic indices (PSV, PSE and NTI) were not correlated with NRI, nor with liana diversity or density (stem and ramet number, basal area) (all  $p > 0.18$ ), but PSV and  $PSE_{ramet}$  were correlated ( $r = 0.5$ ,  $p = 0.018$ ). For PSE and NTI phylogenetic clustering increased with higher density of small tree stems (2 to  $> 10$  cm dbh). Slope, elevation, soil and bamboo density were also selected into the models. The coefficients for slope and elevation had the same direction as found for NRI, but opposite direction for soil PCA axis 1. Tree basal area, which was an important predictor for NRI, was only included as predictor for  $PSE_{ba}$  and had opposite trend as found for NRI: with increasing tree basal area communities become more overdispersed. For PSV, which is based on presence/absence data, phylogenetic overdispersion of liana communities increased with bamboo density, however variation explained by the model was low ( $r^2 = 0.19$ ) (Table 2).

## Discussion

### Phylogenetic structure and disturbance

Species richness and relatedness of lianas (NRI) increased with increasing tree basal area. High tree basal area can be a proxy for low disturbance levels, as an increase in basal area requires that individuals of the tree community have had time to mature (Niklas et al. 2003). Tree basal area usually

increases towards late succession in tropical forests, however it might reach asymptotes in old growth forests (Guariguata and Ostertag 2001, Whitfeld et al. 2012). Abiotic factors such as topography and soil also influenced liana communities. The phylogenetic pattern of NRI found in our study is opposite to the trend found for trees in (sub) tropical forest, where overdispersion increased with forest age (Letcher 2010, Ding et al. 2012, Letcher et al. 2012, Norden et al. 2012 but see Uriarte et al. 2010), and it is in contrast to the findings in other successional systems such as shrub land, old fields and lakes (Verdú and Pausas 2007, Dinnage 2009, Helmus et al. 2010). Whitfeld et al. (2012) found an increasing overdispersion (MPD) of tropical trees with increasing tree basal area, along a succession gradient of similar length to ours (basal area  $4\text{--}40\text{ m}^2\text{ ha}^{-1}$ ). Our prediction was partly fulfilled: liana communities in old growth forest were phylogenetically more clustered, but the linear trend towards phylogenetic overdispersion with decreasing tree basal area deviated from our uni-modal prediction. The interpretation of the phylogenetic pattern should be taken with some caution since the additional indices could not support the relationship of increasing tree basal area and phylogenetic clustering. NRI (or MPD) was used in all mentioned studies except two (Dinnage 2009, Helmus et al. 2010), and is therefore the most comparable index; it remains open if PSE or PSV would have shown the same trends as NRI in these studies.

The clustered phylogenetic patterns of NRI arose from an increase in sister taxa within genera or families all over the

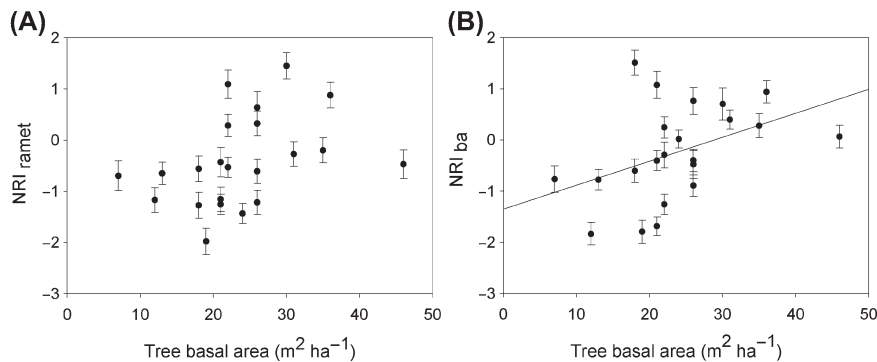


Figure 4. Relationship between net relatedness index (NRI) and tree basal area (Pearson correlation, (A):  $r = 0.38$ ,  $p = 0.079$ , (B):  $r = 0.42$ ,  $p = 0.049$ ). Tree basal area was the independent variable with the highest standard coefficient in an OLS model. For each plot, 100 NRIs based on 100 phylogenies with different branch length were calculated. Shown are means and standard deviation.

Table 2. Results of ordinary least square model (OLS) selection (based on Akaike information criterion) for liana phylogenetic species variability (PSV), phylogenetic species evenness (PSE) and nearest taxon index (NTI). The overall model results (adjusted  $r^2$ , F-ratio, and p-value) and the standardized coefficient and associated p-value for each selected independent variable are given. Transformations of independent variables are indicated in brackets. NTI and PSE are the weighted by ramet density and basal area (ramet, ba). OLS models were run for the averaged NTI, PSV and PSE obtained from 100 different, but equally likely phylogenies.

Independent variable	Response variable									
	PSV		PSE <sub>ramet</sub>		PSE <sub>ba</sub>		NTI <sub>ramet</sub>		NTI <sub>ba</sub>	
	adj. $r^2$ = 0.19, F = 4.3, p = 0.042		adj. $r^2$ = 0.3, F = 4.0, p = 0.036		adj. $r^2$ = 0.54, F = 8.5, p = 0.001		adj. $r^2$ = 0.25, F = 3.7, p = 0.04		adj. $r^2$ = 0.33, F = 3.9, p = 0.026	
	std coef	p	std coef	p	std coef	p	std coef	p	std coef	p
tree basal area					0.306	0.064				
tree stem $\geq$ 10 cm										
tree stem $\geq$ 2 < 10 cm (quadratic)			-0.344	0.092	-0.343	0.041	0.366	0.077	0.363	0.072
canopy closure (log)										
slope							0.419	0.046	0.340	0.084
elevation									-0.452	0.029
soil PCA axis 1					-0.616	0.001				
soil PCA axis 2										
soil PCA axis 3										
bamboo stems (log + 1)	0.437	0.043	0.391	0.058						

phylogeny (Supplementary material Appendix 1, Fig. A7, A8). In old growth forest, more species and congeners were able to coexist. Therefore, phylogenetic patterns were not related to few overrepresented clades with certain ecological or physiological characteristics suitable for establishment in mature forest, but seem to indicate lack of competitive exclusion between sister taxa, or convergence of species with similar traits on similar habitat (environmental filtering). A possible explanation may be the dependence of many liana species on gaps for establishment (Schnitzer and Carson 2001). In old growth forest, where gaps occur scattered, lianas might grow spatially more isolated and therefore lack direct interactions, which might allow coexistence of closely related species. In a more open environment like young forest regrowth, species could spread more evenly across the landscape, leading to more intense competitive interactions and a phylogenetically overdispersed community. This may also explain why liana diversity was higher in old growth forest: more species may be able to co-exist in old growth forest due to spatial isolation of suitable habitat for regeneration (gaps), in combination with dispersal limitation. Previous studies found a variety of diversity patterns for lianas during succession or disturbance, also reduced diversity in disturbed or secondary forests (Yuan et al. 2009, Addo-Fordjour et al. 2012), which is in accordance with our findings. Clustered phylogenetic patterns can also result from competitive exclusion: closely related species with conserved traits might be more successful in outcompeting other community members, for example by being taller (Mayfield and Levine 2010). Increased phylogenetic clustering of communities with ongoing succession was already found in previous studies of woody plants (temperate forest, shrub land) and interpreted as competitive exclusion, e.g. pioneer species get excluded with increasing forest age (Verdú et al. 2009, Kunstler et al. 2012). Due to the clustering of congeners all over the phylogeny, this interpretation is unlikely to apply to our findings.

A second explanation for our findings is that increasing NRI values are an artifact of increasing species richness,

even though phylogenetic indices should be independent of a direct species richness effect (Schweiger et al. 2008). A previous study of fallow land communities and a modeling approach examining disturbance gradients and community phylogenetic structure found that species richness was correlated to some of the phylogenetic indices (Dinnage 2009, Mason and Pavoine 2013). Therefore we checked if random created communities from our dataset showed an increase of NRI with species richness (details see Supplementary material Appendix 1, Fig. A5). We found no correlation, indicating that the pattern in our data is not a mere product of diverse communities saturating the phylogeny.

Including additional indices (NTI, PSE, PSV) which represent slightly different aspects of the phylogenetic community structure uncovered additional, sometimes opposing patterns compared to NRI. NTI is sensitive to changes in terminal clade topology and detects interaction of closely related species. NTI and NRI often have similar trends (Kooyman et al. 2011, Pei et al. 2011, Ding et al. 2012, González-Caro et al. 2012, Letcher et al. 2012). Differences in pattern of NTI and NRI as found in our study, can indicate that biotic interaction, environment and random events shape the communities simultaneously. PSV, which is based on presence/absence data, presents the pure phylogenetic pattern of a community and is sensitive to occurrence of rare species (Helmus et al. 2007). Including abundance data may provide insight into the ecological arrangement in a community (Hardy and Senterre 2007): common species have more influence on the index than species with single individuals, that might occur stochastically or have no competitive power (Vamosi et al. 2009). In the present study, PSV and PSE weighted by ramet density were correlated, but not PSE weighted by basal area, due to the big differences in basal area between species. This emphasizes the importance of considering not only numbers of individuals as abundance but also measurements related to size, which should influence competition.

We focused on liana communities; however interactions that might shape the phylogenetic pattern of a community occur among all (woody) plants in a forest. Lianas compete with trees for underground resources and light (Schnitzer et al. 2005), and share pathogens or pollinators etc. If trees were included in the analysis, the patterns in liana communities would be obscured by the higher abundance and basal area of trees. We also only possessed barcode data for the liana species and including the tree species would have resulted in a more poorly resolved phylogeny, potentially harming our analyses. Future studies should examine the phylogenetic structure of communities during succession, combining and separating different growth forms.

We found no clear pattern in liana abundance along the disturbance gradient, in contrast to numerous other studies that considered succession or disturbance (Dewalt et al. 2000, Letcher and Chazdon 2009, Yuan et al. 2009). However, our finding support a growing number of publications, that found no difference in liana abundance in disturbed and undisturbed tropical forests (Mascaro et al. 2004, Addo-Fordjour et al. 2012, Mo et al. 2013), or higher abundance in undisturbed forest (Addo-Fordjour et al. 2009). The highest liana abundance in our plots occurred in a highly disturbed forest, but the differences in abundance was high between disturbed forest plots. The degree of disturbance and the range of the gradient are hard to compare between studies of different forests and land-use histories. The limited influence of disturbance on liana communities in some of our plots could also result from constant small-scale wood extraction and harvest of non-timber products.

### Influence of multiple phylogenetic trees

Our approach to use 100 phylogenies made the variation of NRI, which results from different branch lengths, visible. Different phylogenies resulted in different sets of selected environmental variables for  $NRI_{\text{basal area}}$ , but not for  $NRI_{\text{ramet}}$ , and therefore can change the interpretation of what is influencing the community assembly. However, it did not make a difference whether NRI was calculated from 100 phylogenies and averaged or from phylogenies of other methods (Bayesian consensus tree and maximum likelihood). By accounting for different, but equally likely, phylogenetic solutions in our NRI calculations, we could reliably relate an increase in tree basal area to more phylogenetically clustered liana communities.

### Utility of liana barcoding

The use of DNA barcoding confirmed species identity of study specimens that could be compared to herbarium collections and made it possible to include specimens that did not have reliable diagnostic morphological characters. Less than 0.7% of all lianas individuals remained unidentified. This highlights the utility of DNA approaches in identifying species with difficult access. Two uncertainties arose while identifying stems only through barcoding of the cambium: zero distance between two sequences could mean that a (stem) sample is ambiguous to several closely related species, but only one of these species is actually present in the database (false positive

identification, Ross et al. 2008). This uncertainty, however, should not affect the calculation of the community phylogenetic structure. Second, in our study the threshold to distinguish between two species was low (pairwise distance  $matK \geq 0.009$ ,  $\geq 0.03 ITS$ ), but it affected only few individuals (8%, Supplementary material Appendix 1, Table A3). Nevertheless, we justify this threshold based on the secondary support of distinct morphological features of the stems.

*Acknowledgements* – We are thankful to M. Fougere and Y. Surget-Groba for advice on the molecular lab work and to Lu Yun for field assistance. The research was financed by the Chinese Academy of Science and the National Natural Science Foundation China (Research Fund for International Young Scientists, grant number 31150110468).

### References

- Addo-Fordjour, P. et al. 2009. Effects of human disturbances and plant invasion on liana community structure and relationship with trees in the Tinte Bepo forest reserve, Ghana. – *For. Ecol. Manage.* 258: 728–734.
- Addo-Fordjour, P. et al. 2012. Effects of human disturbance on liana community diversity and structure in a tropical rainforest, Malaysia: implication for conservation. – *J. Plant Ecol.* 5: 391–399.
- Backlund, M. et al. 2000. Phylogenetic relationships within the Gentianales based on *ndff* and *rbcL* sequences, with particular reference to the Loganiaceae. – *Am. J. Bot.* 87: 1029–1043.
- Beckschäfer, P. et al. 2013. Mapping leaf area index in subtropical upland ecosystems using RapidEye imagery and the random-Forest algorithm. – *iForest* 6: 353–363.
- Dewalt, S. J. et al. 2000. Density and diversity of lianas along a chronosequence in a central Panamanian lowland forest. – *J. Trop. Ecol.* 16: 1–19.
- Ding, Y. et al. 2012. Disturbance regime changes the trait distribution, phylogenetic structure and community assembly of tropical rain forests. – *Oikos* 121: 1263–1270.
- Dinnage, R. 2009. Disturbance alters the phylogenetic composition and structure of plant communities in an old field system. – *PLoS One* 4: e7071.
- Felsenstein, J. 1984. Phylogenies and the comparative method. – *Am. Nat.* 125: 1–15.
- Fleischer, K. 1990. Stratified sampling using double samples. – *Stat. Pap.* 63: 55–63.
- Gerwing, J. J. et al. 2006. A standard protocol for liana censuses. – *Biotropica* 38: 256–261.
- Gonzalez, M. A. et al. 2009. Identification of Amazonian trees with DNA barcodes. – *PLoS One* 4: e7483.
- González-Caro, S. et al. 2012. Sensitivity of metrics of phylogenetic structure to scale, source of data and species pool of hummingbird assemblages along elevational gradients. – *PLoS One* 7: e35472.
- Gotelli, N. J. and Colwell, R. K. 2001. Quantifying biodiversity: procedures and pitfalls in the measurement and comparison of species richness. – *Ecol. Lett.* 4: 379–391.
- Guariguata, M. R. and Ostertag, R. 2001. Neotropical secondary forest succession: changes in structural and functional characteristics. – *For. Ecol. Manage.* 148: 185–206.
- Hardy, O. J. and Senterre, B. 2007. Characterizing the phylogenetic structure of communities by an additive partitioning of phylogenetic diversity. – *J. Ecol.* 95: 493–506.
- Helmus, M. R. et al. 2007. Phylogenetic measures of biodiversity. – *Am. Nat.* 169: E68–E83.
- Helmus, M. R. et al. 2010. Communities contain closely related species during ecosystem disturbance. – *Ecol. Lett.* 13: 162–174.
- Kajita, T. et al. 2001. *rbcL* and legume phylogeny, with particular reference to Phaseoleae, Millettieae, and allies. – *Syst. Bot.* 26: 515–536.

- Kembel, S. W. 2009. Disentangling niche and neutral influences on community assembly: assessing the performance of community phylogenetic structure tests. – *Ecol. Lett.* 12: 949–960.
- Kembel, S. W. et al. 2010. Picante: R tools for integrating phylogenies and ecology. – *Bioinformatics* 26: 1463–1464.
- Kooyman, R. et al. 2011. Phylogenetic tests of community assembly across regional to continental scales in tropical and subtropical rain forests. – *Global Ecol. Biogeogr.* 20: 707–716.
- Kress, W. J. et al. 2009. Plant DNA barcodes and a community phylogeny of a tropical forest dynamics plot in Panama. – *Proc. Natl Acad. Sci. USA* 106: 18621–18626.
- Kunstler, G. et al. 2012. Competitive interactions between forest trees are driven by species' trait hierarchy, not phylogenetic or functional similarity: implications for forest community assembly. – *Ecol. Lett.* 15: 831–840.
- Larkin, M. A. et al. 2007. Clustal W and Clustal X version 2.0. – *Bioinformatics* 23: 2947–2948.
- Laurance, W. F. et al. 2001. Rainforest fragmentation and the structure of Amazonian liana communities. – *Ecology* 82: 105–116.
- Letcher, S. G. 2010. Phylogenetic structure of angiosperm communities during tropical forest succession. – *Proc. R. Soc. B* 277: 97–104.
- Letcher, S. G. and Chazdon, R. L. 2009. Lianas and self-supporting plants during tropical forest succession. – *For. Ecol. Manage.* 257: 2150–2156.
- Letcher, S. G. et al. 2012. Phylogenetic community structure during succession: evidence from three Neotropical forest sites. – *Perspect. Plant Ecol. Evol. Syst.* 14: 79–87.
- Livshultz, T. et al. 2007. Phylogeny of Apocynoideae and the APSA clade (Apocynaceae S.L.). – *Ann. Missouri Bot. Gard.* 94: 324–359.
- Maddison, W. P. and Maddison, D. R. 2011. Mesquite: a modular system for evolutionary analysis. – Version 2.75.
- Mascaro, J. et al. 2004. Liana diversity, abundance, and mortality in a tropical wet forest in Costa Rica. – *For. Ecol. Manage.* 190: 3–14.
- Mason, N. W. H. and Pavoine, S. 2013. Does trait conservatism guarantee that indicators of phylogenetic community structure will reveal niche-based assembly processes along stress gradients? – *J. Veg. Sci.* 24: 820–833.
- Mayfield, M. M. and Levine, J. M. 2010. Opposing effects of competitive exclusion on the phylogenetic structure of communities. – *Ecol. Lett.* 13: 1085–1093.
- Mo, X.-X. et al. 2013. Change in phylogenetic community structure during succession of traditionally managed tropical rainforest in southwest China. – *PLoS One* 8: e71464.
- Niklas, K. J. et al. 2003. Tree size frequency distributions, plant density, age and community disturbance. – *Ecol. Lett.* 6: 405–411.
- Norden, N. et al. 2012. Demographic drivers of successional changes in phylogenetic structure across life-history stages in plant communities. – *Ecology* 93: 70–82.
- Oksanen, J. et al. 2013. Package “vegan”. Community ecology package, version 2.0-9. – <<http://cran.r-project.org/package=vegan>>.
- Pei, N. et al. 2011. Exploring tree-habitat associations in a Chinese subtropical forest plot using a molecular phylogeny generated from DNA barcode loci. – *PLoS One* 6: e21273.
- Prinzinger, A. et al. 2001. The niche of higher plants: evidence for phylogenetic conservatism. – *Proc. Biol. Sci.* 268: 2383–2389.
- Rangel, T. F. et al. 2010. SAM: a comprehensive application for Spatial Analysis in Macroecology. – *Ecography* 33: 46–50.
- Ronquist, F. et al. 2012. MrBayes 3.2: efficient Bayesian phylogenetic inference and model choice across a large model space. – *Syst. Biol.* 61: 539–542.
- Ross, H. A. et al. 2008. Testing the reliability of genetic methods of species identification via simulation. – *Syst. Biol.* 57: 216–230.
- Schnitzer, S. A. and Carson, W. P. 2001. Treefall gaps and the maintenance of species diversity in a tropical forest. – *Ecology* 82: 913–919.
- Schnitzer, S. A. and Bongers, F. 2002. The ecology of lianas and their role in forests. – *Trends Ecol. Evol.* 17: 223–230.
- Schnitzer, S. A. and Bongers, F. 2011. Increasing liana abundance and biomass in tropical forests: emerging patterns and putative mechanisms. – *Ecol. Lett.* 14: 397–406.
- Schnitzer, S. A. et al. 2000. The impact of lianas on tree regeneration in tropical forest canopy gaps: evidence for an alternative pathway of gap-phase regeneration. – *J. Ecol.* 88: 655–666.
- Schnitzer, S. A. et al. 2005. Disentangling above- and below-ground competition between lianas and trees in a tropical forest. – *J. Ecol.* 93: 1115–1125.
- Schnitzer, S. A. et al. 2008. Supplemental protocol for liana census. – *For. Ecol. Manage.* 255: 1044–1049.
- Schweiger, O. et al. 2008. A comparative test of phylogenetic diversity indices. – *Oecologia* 157: 485–495.
- Stamatakis, A. 2006. RAxML-VI-HPC: maximum likelihood-based phylogenetic analyses with thousands of taxa and mixed models. – *Bioinformatics* 22: 2688–2690.
- Swenson, N. G. et al. 2012. Temporal turnover in the composition of tropical tree communities: functional determinism and phylogenetic stochasticity. – *Ecology* 93: 490–499.
- Tamura, K. et al. 2011. MEGA5: molecular evolutionary genetics analysis using maximum likelihood, evolutionary distance, and maximum parsimony methods. – *Mol. Biol. Evol.* 28: 2731–2739.
- Uriarte, M. et al. 2010. Trait similarity, shared ancestry and the structure of neighbourhood interactions in a subtropical wet forest: implications for community assembly. – *Ecol. Lett.* 13: 1503–1514.
- Vamosi, S. M. et al. 2009. Emerging patterns in the comparative analysis of phylogenetic community structure. – *Mol. Ecol.* 18: 572–592.
- Verdú, M. and Pausas, J. G. 2007. Fire drives phylogenetic clustering in Mediterranean Basin woody plant communities. – *J. Ecol.* 95: 1316–1323.
- Verdú, M. et al. 2009. Phylogenetic signatures of facilitation and competition in successional communities. – *J. Ecol.* 97: 1171–1180.
- Webb, C. O. 2000. Exploring the phylogenetic structure of ecological communities: an example for rain forest trees. – *Am. Nat.* 156: 145–155.
- Webb, C. O. et al. 2002. Phylogenies and community ecology. – *Annu. Rev. Ecol. Syst.* 33: 475–505.
- Whitfeld, T. J. S. et al. 2012. Change in community phylogenetic structure during tropical forest succession: evidence from New Guinea. – *Ecography* 35: 821–830.
- WRB IUSS Working Group 2006. World reference base for soil resources. – World Soil Resources Report no. 103.
- Xu, J. et al. 2009. Functional links between biodiversity, livelihoods, and culture in a Hani swidden landscape in southwest China. – *Ecol. Soc.* 14: 20.
- Xu, J. et al. 2014. Landscape transformation through the use of ecological and socioeconomic indicators in Xishuangbanna, southwest China, Mekong Region. – *Ecol. Indicators* 36: 749–756.
- Yuan, C. et al. 2009. Species composition, diversity, and abundance of lianas in different secondary and primary forests in a subtropical mountainous area, SW China. – *Ecol. Res.* 24: 1361–1370.
- Zhang, S. et al. 2011. Multi-gene analysis provides a well-supported phylogeny of Rosales. – *Mol. Phylogenet. Evol.* 60: 21–28.
- Zhu, H. et al. 2005. Species composition, physiognomy and plant diversity of the tropical montane evergreen broad-leaved forest in southern Yunnan. – *Biodivers. Conserv.* 14: 2855–2870.
- Zhu, H. et al. 2006. Species composition and biogeography of tropical montane rain forest in southern Yunnan of China. – *Gard. Bull. Singapore* 58: 81–132.

Supplementary material (Appendix ECOG-01051 at <[www.ecography.org/readers/appendix](http://www.ecography.org/readers/appendix)>). Appendix 1.